



Rechargeable lithium sulfide electrode for a polymer tin/sulfur lithium-ion battery

Jusef Hassoun^a, Yang-Kook Sun^b, Bruno Scrosati^{a,b,*}

^a Department of Chemistry, University of Rome Sapienza, 00185 Rome, Italy

^b Department of Energy Engineering, Hanyang University, Seoul 133-792, South Korea

ARTICLE INFO

Article history:

Received 12 May 2010

Received in revised form 26 June 2010

Accepted 28 June 2010

Available online 14 August 2010

Keywords:

Lithium sulfide

Cathode

Polymer lithium-ion battery

ABSTRACT

In this work we investigate the electrochemical behavior of a new type of carbon–lithium sulfide composite electrode. Results based on cyclic voltammetry, charge (lithium removal)–discharge (lithium acceptance) demonstrate that this electrode has a good performance in terms of reversibility, cycle life and coulombic efficiency. XRD analysis performed in situ in a lithium cell shows that lithium sulfide can be converted into sulfur during charge and re-converted back into sulfide during the following discharge process. We also show that this electrochemical process can be efficiently carried out in polymer electrolyte lithium cells and thus, that the $\text{Li}_2\text{S}-\text{C}$ composite can be successfully used as cathode for the development of novel types of rechargeable lithium-ion sulfur batteries where the reactive and unsafe lithium metal anode is replaced by a reliable, high capacity tin–carbon composite and the unstable organic electrolyte solution is replaced by a composite gel polymer membrane that is safe, highly conductive and able to control dendrite growth across the cell. This new $\text{Sn}-\text{C}/\text{Li}_2\text{S}$ polymer battery operates with a capacity of 600 mAh g^{-1} and with an average voltage of 2 V, this leading to a value of energy density amounting to 1200 Wh kg^{-1} .

© 2010 Elsevier B.V. All rights reserved.

1. Introduction

In view of application in emerging key markets, such as energy renewal and sustainable road transport, new and high performance storage systems are urgently needed. Lithium-ion batteries may be the power sources of choice for automobile application. However, the state-of-art lithium batteries, based on the graphite/lithium cobalt combination, still requires considerable progress to meet the stringent requirements of these emerging markets: increase in energy storage, efficient control of safety and a shift to cost-effective electrode and electrolyte materials, are mandatory steps. To meet these stringent demands, new, revolutionary avenues must be explored.

A valid example is provided by the lithium–sulfur battery that exploits a basic electrochemical process: $16\text{Li} + \text{S}_8 \rightleftharpoons 8\text{Li}_2\text{S}$ that, assuming full conversion, gives theoretical specific energy and energy density values of 2600 Wh kg^{-1} and 2800 Wh l^{-1} , respectively. These values are much greater than those possibly attainable with any conventional lithium-ion battery. In addition sulfur is

a cheap and abundantly available material and thus, the cost of lithium sulfur batteries is expected to be low.

Several issues, however, have so far prevented the practical development of this important lithium battery system [1]. They mainly include: the insulating nature of sulfur (that limits the battery rate); the high solubility of the discharge products (that affects cycle life) and the high reactivity of the lithium metal anode (that induces safety risk). In the attempt to solve these issues, the Li/S battery has been investigated by many workers for several decades [2–13]. However, although progress has been achieved, no real breakthrough has been so far obtained, also because the most of the studies above cited have been limited to a conventional cell configuration consisting of sulfur as the positive electrode, lithium metal as the negative electrode and a solution of a lithium salt in aprotic organic solvents as the electrolyte.

In a previous paper [14] we reported an advanced version of the lithium–sulfur battery system exploiting a totally new electrochemical concept based on the replacement of all the three cell elements, namely anode, cathode and electrolyte. We demonstrated that this concept led to a unique lithium-ion sulfur battery offering major advantages in terms of energy density, reliability and safety. In this work we continue the investigation of this new battery by studying in detail its performance in terms of the basic electrochemistry of the cathode material.

* Corresponding author at: Department of Chemistry, University of Rome Sapienza, Piazzale Aldo Moro 5, 00185 Rome, Italy.

E-mail address: bruno.scrosati@uniroma1.it (B. Scrosati).

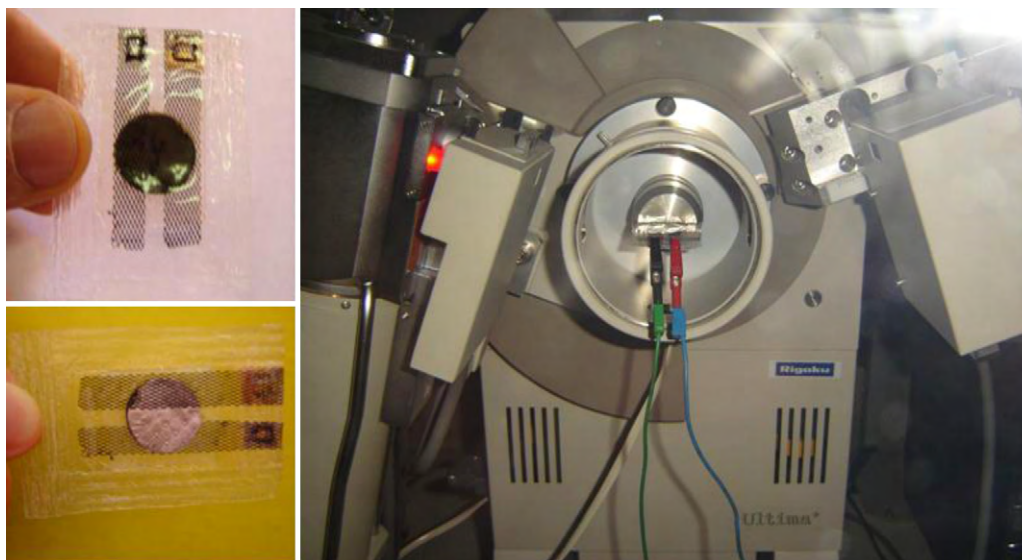


Fig. 1. Instrumental setup used for the in situ XRD measurements.

2. Experimental

2.1. Li_2S -C electrode

The Li_2S -C electrode was prepared by Low Energy Glass Ball Milling (LEGBM) by blending, under an argon atmosphere, pure crystalline lithium sulfide (Li_2S , Aldrich) and Super P carbon (SP), in a 1:1 weight ratio. The sieved and dried components were introduced inside sealed, polyethylene bottles where they were intimately mixed by ball-milling for at least 24 h to obtain a homogeneous powder mixture. The Li_2S -C electrode was then fabricated in a form of thin film by hot pressing on a $15\ \mu\text{m}$ aluminum foil support a blend formed by 70% Li_2S -C (active material) and 30% $\text{PEO}_{20}\text{LiCF}_3\text{SO}_3$ (binder).

2.2. The Sn-C electrode

The Sn-C electrode was prepared following the procedure described in details in previous works [15,16]. Basically, the synthesis involved the infiltration of an organometallic tin precursor tributylphenyltin (TBPT) in an organic Resorcinol (benzene-1,3-diol)-formaldehyde (methanal) gel, followed by calcination under argon. Particular care was taken to assure the purity of the final product and, in particular, to prevent its oxidation in the course of the synthesis. Also this electrode was fabricated in the form of a thin film by doctor-blade deposition on a copper substrate of a slurry composed of 80% Sn-C (active material), 10% PVdF 6020, Solvay Solef (binder) and 10% SP carbon (electronic support).

2.3. The PEO-based gel electrolyte

The PEO-based gel polymer electrolyte was formed by following a solvent-free procedure optimized in our laboratory [17]. Linear poly(ethylene oxide), PEO (Aldrich), having a molecular mass of 6×10^5 , was dried under vacuum at 50°C for 24 h before use. Nanoscale ZrO_2 (Aldrich) ceramic filler was dried under vacuum at 300°C for 24 h. LiCF_3SO_3 (Aldrich, Battery Grade product) was used as received. The polymer electrolyte components, namely poly(ethylene oxide) PEO, the LiCF_3SO_3 lithium salt and the ZrO_2 ceramic filler, were carefully sieved and only the smallest particle size fractions were used. The sieved and dried components were introduced, in the composition of $\text{PEO}_{20}\text{LiCF}_3\text{SO}_3$ - ZrO_2 10% weight

percent, inside sealed, polyethylene bottles and there intimately mixed by ball-milling for at least 24 h to obtain a homogeneous powder mixture. The mixture was then hot-pressed in an aluminum mold at a temperature of 90°C and at 0.5 tons for 15 min and then at 4 tons for 45 min. The polymer electrolyte membrane was stored under argon. The final gel polymer electrolyte was formed by swelling for 10 min the $\text{PEO}_{20}\text{LiCF}_3\text{SO}_3$ -10% S - ZrO_2 membrane with standard LP30 (Merck) battery grade solution (dimethyl carbonate, EC:DMC, 1:1, LiPF_6 1 M) saturated by Li_2S .

2.4. The in situ XRD analysis

The structural variation during galvanostatic charge of the electrode was controlled by X-Ray Diffraction (XRD), using a D-max Ultima + Rigaku diffractometer with $\text{Cu-K}\alpha$ radiation. A transparent plastic cell, coupling Li_2S -C electrode pressed into Al-grid with the polymer electrolyte and metallic lithium, was assembled under argon atmosphere, sealed, and used as testing sample to be inserted in the XRD instrument. The cell was submitted to a full charge-discharge cycle, driven and controlled by Maccor battery cycler. The cycling test was interrupted at various stages of the process and XRD taken in situ in order to detect the status of charge and discharge. Fig. 1 illustrates the experimental setup.

2.5. The electrochemical measurement

The cyclic voltammetry was performed at a $100\ \mu\text{V s}^{-1}$ rate and within a 1.5–4.1 V voltage limit using a PAR 362 potentiostat. A three-electrode cell, having Li_2S -C as the working electrode and lithium metal as counter and reference electrode, was used for this test. The charge-discharge tests were carried out in a galvanostatic mode in two-electrode cells using either lithium metal or tin-carbon composite as the anode. The cycling protocol was run and controlled by a Maccor Series 4000 Battery Test System instrument. The impedance spectroscopy analysis was carried out with an amplitude of 10 mV in a 75 kHz to 0.1 Hz frequency range using a Versastat Ametek controlling instrument.

2.6. The cell prototypes

All the cell prototypes were assembled in 1.0 cm diameter T-shaped cases. The cells were prepared by placing the gel polymer

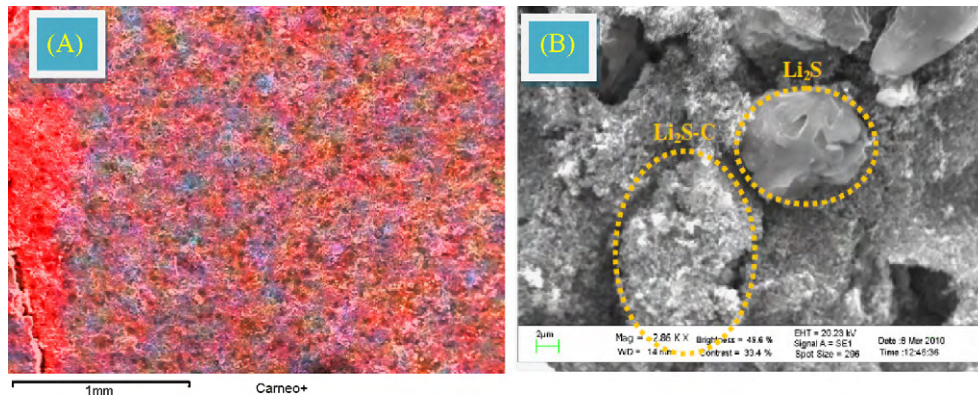


Fig. 2. EDS (A) and SEM (B) images of the $\text{Li}_2\text{S-C}$ cathode material developed in this work. In the Cameo in (A), red is carbon and blue is Li_2S . (For interpretation of the references to color in this figure legend, the reader is referred to the web version of the article.)

membrane as electrolyte separator in between 1.0 cm diameter electrode disks ($\text{Li/Li}_2\text{S-C}$ or $\text{Sn-C/Li}_2\text{S-C}$). The charge–discharge cycling response was run and controlled by a Maccor Series 4000 Battery Test System instrument.

3. Results and discussion

The battery developed in our laboratory is fabricated in the “discharged” state by using a carbon–lithium sulfide, $\text{C-Li}_2\text{S}$, composite as the cathode (14). Fig. 2 shows the EDS–SEM images of this cathode. Image A illustrates the average distribution of carbon and lithium sulfide throughout the electrode bulk. The image B shows the Li_2S particle size and it reveals that, while the majority of these particles are covered by carbon, there are still few that remain uncovered. This may be an issue in terms of appropriate battery operation and thus, optimization of the morphology of the cathode may eventually need to be addressed.

To overcome one of the major obstacles of “conventional” lithium sulfur batteries, i.e., the high solubility in common organic electrolytes of the poly sulfides Li_2S_x ($1 \leq x \leq 8$) that form as intermediates during both charge and discharge processes, we have replaced the conventional liquid electrolyte with a gel-type polymer membrane, formed by trapping into a poly(ethylene oxide)–trifluoromethanesulfonate, $\text{PEO-LiCF}_3\text{SO}_3$ polymer matrix a liquid solution of lithium hexafluorophosphate, LiPF_6 in a ethylene carbonate–dimethylcarbonate, EC-DMC mixture added by lithium sulfide to saturation [14]. We also dispersed into the mixture a zirconia ceramic filler to enhance the mechanical properties of the gel and to improve liquid retention within its bulk [18,19]. For simplicity sake, we may hereafter refer to this composite gel polymer electrolyte with the acronym CGPE. It is expected that the external polymer layer may act as a physical barrier to the direct contact of the electrode components with the internal liquid solution, this contributing to prevent the dissolution of the sulfide anions from the cathode, as well as the attack of the same anions to the anode. Furthermore, the addition up to saturation of lithium sulfide in the liquid component leads to a combined physical and chemical barrier to block most of the dissolution processes, as indeed previously demonstrated [14]. Finally, the replacement of the common liquid electrolyte solution with an advanced lithium conducting membrane confers to the battery all those advantages that are typical of a plastic configuration, such as absence of leaking, easy fabrication procedure and modular design.

This $\text{Li/CGPE/Li}_2\text{S}$ cell may be activated by a “charge” process, involving the conversion of lithium sulfide to lithium and sulfur, namely by an electrochemical process that may be basically indicated as: $8\text{Li}_2\text{S} \rightarrow 16\text{Li} + \text{S}_8$, although its development may involve a sequence of intermediate polysulfides Li_2S_x ($1 \leq x \leq 8$). The nature of

the process and its completion are confirmed by Fig. 3 that reports the XRD analysis obtained “in situ” in the course of various stages of the charge process.

Fig. 3A illustrates the voltage profile of the galvanostatic charge process and shows the points at which the charge current was interrupted and the XRD analysis of the electrode was taken. To be noticed that two spikes appears in the voltage profile between points 2 and 3; we may tentatively associate them to dendrite formations at the lithium metal anode surface, occurring in the course of the low rate, galvanostatic charge process. Interestingly, these dendrites did not grow all the way to short the cell but they were blocked and dissolved, as demonstrated by the fact that the volt-

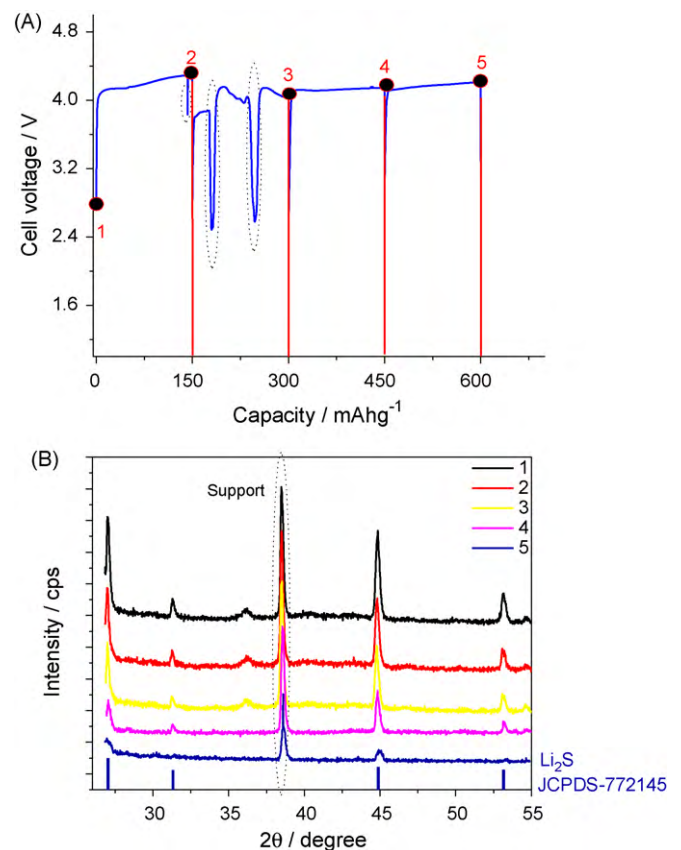


Fig. 3. XRD analysis run “in situ” on a $\text{Li/CGPE/Li}_2\text{S}$ cell at various stages of the charge process. (A) Voltage profile with indication of the points at which the current was interrupted for the XRD analysis. (B) Evolution of the XRD pattern upon ongoing of the process.

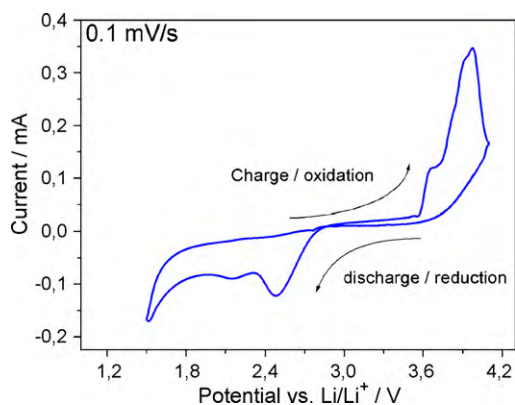


Fig. 4. Cycling voltammetry of the $\text{Li}_2\text{S-C}$ electrode in the GGPE electrolyte. Li counter and reference electrode 50°C . Scan rate: 0.1 mV s^{-1} . CGPE: composite gel polymer electrolyte.

age profile quickly reassumed its normal trend. We think that this dendrite-blocking action is an additional bonus of the polymer electrolyte that, in virtue of its quasi-solid state configuration, acts as a physical barrier to dendrite penetration. Fig. 3B shows the XRD pattern evolution upon proceeding of the charge process. Clearly, the peaks associated with Li_2S (JCPDS-772145) progressively decrease to almost vanish at the end of the charge, this demonstrating that lithium sulfide is in fact consumed during charge. We could not extend the test to lower theta values since in this range the response is totally covered by the signal of the plastic foil support. Although the very low crystallinity of the reaction product has not allowed us to obtain confirmation by XRD, we may reasonably assume that lithium sulfide is converted into sulfur. It is also difficult to carry out the XRD on the discharge re-conversion process due to the amorphous nature of the products obtained in charge. However, this measurement is planned and the best conditions for performing it are under evaluation in our laboratory.

Once charge is completed, the battery may be discharged by reacting the formed sulfur with lithium to reconvert back to lithium sulfide and the entire charge–discharge cycle may be efficiently repeated several times [14]. The reversibility of the process is further supported by Fig. 4, which shows a typical cyclic voltammetry of the $\text{Li}_2\text{S-C}$ electrode and by Fig. 5, which shows a typical charge–discharge cycle of the $\text{Li/CGPE/Li}_2\text{S}$ cell.

As seen in Fig. 4, the anodic scan (i.e., the “charge” of the $\text{Li}_2\text{S-C}$ electrode) develops with a main peak at 3.5–4.0 V versus Li, convoluting the various intermediate steps that characterize in the conversion process from Li_2S to elemental sulfur [1,3]. The electrochemical process is reversed in the following cathodic scan (i.e., the “discharge” of the electrode) where the CV trace reveals a series of

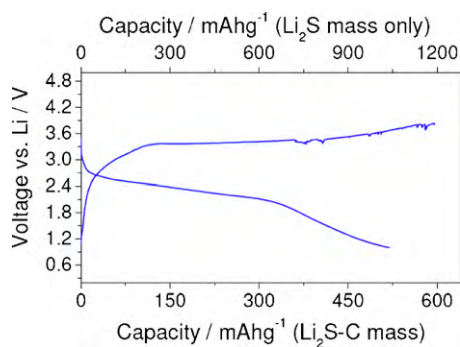


Fig. 5. Typical charge–discharge cycle of the $\text{Li/CGPE/Li}_2\text{S-C}$ cell. Cycling rate: $C/20$ ($1C = 2.2\text{ mA cm}^{-2}$), 60°C . The capacity is quoted both in terms of total electrode mass and in terms of active material mass only. CGPE: composite gel polymer electrolyte.

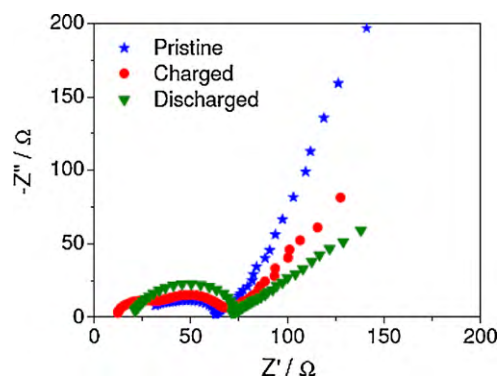


Fig. 6. Impedance response of the $\text{Li}_2\text{S-C}$ electrode in CGPE. The plots refer to the pristine, fully charged and fully discharged, respectively, state. CGPE composite gel polymer electrolyte.

peaks representing the re-conversion of elemental sulfur throughout the intermediate lithium sulfide species [1,3]. The integration of the peaks area reveals that the overall capacity related to the charge process matches that of the discharge process, demonstrating the efficiency of the overall electrochemical reaction.

The reversibility of this reaction is further confirmed by the typical charge–discharge cycle reported in Fig. 5. The voltage profiles are evolving with a sequence of charge and discharge plateaus that correspond to the peaks highlighted by the CV analysis, although at a somewhat lower value compared with Fig. 4. We see that the voltage profiles evolve around 2.5 V versus Li with a total capacity of the order of 600 mAh g^{-1} . The capacity is here calculated on the basis of the $\text{Li}_2\text{S-C}$ electrode mass; if the calculation is referred to the Li_2S mass only, the capacity reaches values of the order of 1200 mAh g^{-1} . The capacity delivered in charge is returned in discharge with a coulombic efficiency approaching 100%, and this further demonstrates the electrochemical feasibility and the reversibility of our $\text{Li}_2\text{S-C}$ electrode material.

The kinetics of the $\text{Li}_2\text{S-C}$ electrode have been examined by impedance spectroscopy. Fig. 6 shows typical impedance plots that compare the response of the electrode at its pristine state, after full charge and after full discharge, respectively. Clearly, the low frequency intercept with the real axis, that represents the electrode/electrolyte interfacial resistance, remains almost unchanged. This leads to the important conclusion that the electrode processes do not induce increase in the resistance of interfacial passivation films, if any, and, in particular, in the charge transfer resistance. This experimental evidence confirms the favorable electrochemical behavior of our $\text{Li}_2\text{S-C}$ electrode that keeps its integrity upon cycling. On the other hand, the impedance curve also reveals that the interfacial resistance is of the order of $60\text{--}70\ \Omega$, a still too high value to assure good rate capabilities. Therefore, efforts to improve the electrode morphology, such as to reduce the ohmic polarization, are in progress in our laboratories.

As already reported in a previous work [14], the chemical composition of the battery is further improved in respect to conventional systems by replacing the reactive lithium metal with a chemically stable, tin–carbon composite Sn-C , 1:1 wt%, to finally form a new type of lithium-ion, polymer, tin–lithium sulfide battery. The choice of this particular Sn-C composite anode was motivated by the fact that previous work carried out in one of our laboratories had demonstrated excellent performance in lithium cells in terms of cycle life, capacity, rate and chemical stability [15,16]. In addition, the specific capacity of Sn-C matches that of the $\text{Li}_2\text{S-C}$, this being very convenient for achieving cell balance when combining the two electrodes in the battery structure.

The electrochemical process of this $\text{Sn-C/CGPE/Li}_2\text{S-C}$ battery is the reversible reaction of the lithium–tin alloy with

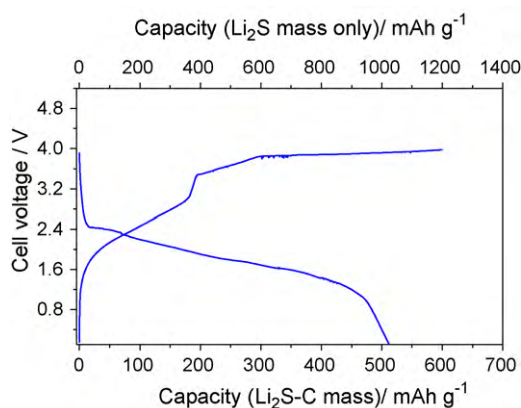


Fig. 7. Typical charge–discharge cycle of the Sn–C/CGPE/Li₂S–C cell. Cycling rate: C/20 (1C = 760 mA g⁻¹ cm⁻²). Room temperature. The capacity is quoted both in terms of total electrode mass and in terms of active material mass only. CPGE: composite gel polymer electrolyte.

elemental sulfur, to form tin metal and lithium sulfide, i.e., $2.2\text{Li}_2\text{S} + \text{Sn-C} \rightleftharpoons \text{Li}_{4.4}\text{Sn} + 2.2\text{S} + \text{C}$ that gives an energy density of the order of 1000 Wh kg⁻¹ or 2000 Wh kg⁻¹, depending whether the mass of Li₂S–C or the mass of the Li₂S active material only, is considered.

Fig. 7 shows a typical voltage profile of a charge–discharge cycle of this Sn–C/CGPE/Li₂S battery. Similarly to the case of the cell using lithium metal as anode, the capacity consumed in charge, i.e., about 600 mAh g⁻¹, approaches that delivered in discharge, this demonstrating that the reversibility of the electrochemical process also holds for the cell where Li metal is replaced by the Sn–C composite.

Fig. 8 illustrates the cycling performance of the Sn–C/CGPE/Li₂S–C polymer battery. We notice that no decay in capacity delivery is observed upon prolonged cycling, e.g., see the results at C/5. This evidence, combined by the fact that the test of Fig. 8 lasted for several days, is a good proof of the stability of our cathode material. These results then confirm the validity of the new lithium-ion battery configuration and that the thereby adopted chemistry effectively prevents the dissolution of lithium sulfide and assures the integrity of the electrode structure upon cycling.

On the other hand, Fig. 8 also shows that the value of the capacity drops consistently by cycling at a relatively high rate, e.g., at C/5; however, the capacity fully recovers when returning to low rate regimes, e.g., at C/10–C/20, suggesting that the electrode kinetics are mainly controlled by an ohmic overvoltage, as already evidenced by the impedance results. Therefore, further work is needed to make this Sn–C/CPGE/Li₂S–C polymer battery fully valid for practical applications. The obvious approach is in the improvement of

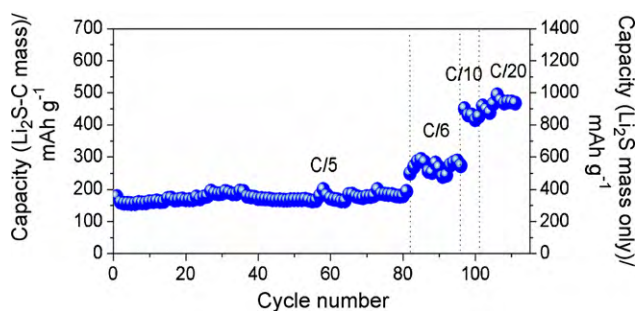


Fig. 8. Capacity versus cycle number of a Sn–C/CPGE/Li₂S–C at different rates, i.e., 152 mA cm⁻² g⁻¹ (C/5); 127 mA cm⁻² g⁻¹ (C/6) and 76 mA cm⁻² g⁻¹ (C/10) and 38 mA cm⁻² g⁻¹ (C/20) rate. The capacity is quoted both in terms of Li₂S–C mass and in terms of Li₂S active material mass only. CPGE: composite gel polymer electrolyte.

the cathode morphology, e.g., by assuring a full carbon coverage of the Li₂S particles. Work in this direction is in fact in progress in our laboratories.

To be noticed that lithium sulfide-based electrodes have been discussed in the past, for example in the form of metal composites, however either in combination with a conventional lithium metal anode [20] or as electrodes alternative to conventional intercalation compounds [21]. Takeuchi et al. [22] have described a lithium–sulfide–carbon composites using spark–plasma–sintering process. These authors showed that their electrode is electrochemically active and suitable for application for rechargeable lithium-ion sulfur cells, this indirectly supporting the results reported in this work. However, also the work of Takeuchi et al. is limited to a study of the Li₂S–C electrochemical response in a lithium metal cells with no attempt to use it in advanced lithium-ion cell configurations. Recently, Cui and co-workers have reported a lithium-ion sulfur battery based on a Li₂S/Si combination [23]. The concept is somehow similar to that here described. However, the life of the battery appears limited to few cycles [23].

4. Conclusion

In synthesis, in this work we have reported a series of experimental evidences that clearly demonstrate the high reversibility and cycling efficiency of our Li₂S–C electrode. We show that by using this Li₂S–C cathode in combination with a tin–carbon composite and a gel-type polymer electrolyte, a new type of tin/sulfur lithium-ion battery having unique characteristics in terms of high capacity, high energy density, safety and projected low cost can be obtained, this confirming data reported in a previous work [14]. The road to make this battery viable for practical application is still long and further improvements are needed. A major one is the optimization of the cathode morphology in order to reduce ohmic polarizations. Results reported in recent lithium battery literature provide some useful suggestions on the route to follow for improving the rate capability of lithium battery electrodes. Work is in progress to test whether these approaches are also beneficial for our lithium sulfide electrode.

Acknowledgement

This work was carried out within the SIID Project “REALIST” sponsored by Italian Institute of Technology. This research was also supported by WCU (World Class University) program through the Korea Science and Engineering Foundation by Education, Science, and Technology (R31-2008-000-10092)

References

- [1] H.-J. Ahn, K.-W. Kim, J.-H. Ahn, Lithium Sulfur Cells, Encyclopedia of Power Sources, Elsevier, 2009, pp. 155–161.
- [2] R.D. Rauh, K.M. Abraham, G.F. Pearson, J.K. Suprenant, S.B. Brummer, J. Electrochem. Soc. 126 (1979) 523–527.
- [3] E. Peled, H. Yamin, J. Power Sources 9 (1983) 281–287.
- [4] D. Peramunage, S.A. Licht, Science 261 (1993) 1029–1032.
- [5] J. Shim, K.A. Stribel, E.J. Cairns, J. Electrochem. Soc. 149 (2002) A1321–A1325.
- [6] D. Aurbach, E. Pollak, R. Elazari, G. Salitra, C.S. Kelley, J. Affinito, J. Electrochem. Soc. 156 (2009) A694–A702.
- [7] S.-E. Cheon, K.-S. Ko, J.-H. Cho, S.-W. Kim, E.-Y. Chin, H.-T. Kim, J. Electrochem. Soc. 150 (2003) A800–A805.
- [8] J.-W. Choi, J.-K. Kim, G. Cheruvally, J.-H. Ahn, K.-W. Kim, Electrochim. Acta 52 (2007) 2075–2082.
- [9] J.H. Shin, E.J. Cairns, J. Electrochem. Soc. 155 (2008) A368–A373.
- [10] H.-S. Ryu, H.-J. Ahn, K.-W. Kim, J.-H. Ahn, K.-K. Cho, T.-H. Nam, J.-U. Kim, G.-B. Cho, J. Power Sources 163 (2006) 201–206.
- [11] L.X. Yuan, J.K. Feng, X.P. Ai, Y.L. Cao, S.L. Chen, H.X. Yang, Electrochem. Commun. 8 (2006) 610–614.
- [12] S.S. Jeong, Y.T. Lim, Y.J. Choi, G.B. Cho, K.W. Kim, H.J. Ahn, K.K. Cho, J. Power Sources 174 (2007) 745–750.
- [13] X. Ji, K.T. Lee, L.F. Nazar, Nat. Mater. 8 (2009) 500–506.
- [14] J. Hassoun, B. Scrosati, Angew. Chem. Int. Ed. 49 (2010) 2371–2374.

- [15] G. Derrien, J. Hassoun, S. Panero, B. Scrosati, *Adv. Mater.* 19 (2007) 2336–2340.
- [16] J. Hassoun, G. Derrien, S. Panero, B. Scrosati, *Adv. Mater.* 20 (2008) 3169–3175.
- [17] G.B. Appetecchi, F. Croce, J. Hassoun, B. Scrosati, M. Salomon, F. Cassel, *J. Power Sources* 114 (2003) 105–112.
- [18] B. Scrosati, Lithium polymer electrolytes, in: W.A. van Schalkwijk, B. Scrosati (Eds.), *Advances in Lithium Ion Batteries*, Kluwer Academic/Plenum Publishers, New York, 2002, pp. 251–266.
- [19] G.B. Appetecchi, P. Romagnoli, B. Scrosati, *Electrochem. Commun.* 3 (2001) 281–284.
- [20] A. Hayashi, R. Ohtsubo, T. Ohtomo, F. Mizuno, M. Tatsumisago, *J. Power Sources* 183 (2008) 422–426.
- [21] M.N. Obrovac, J.R. Dahn, *Electrochem. Solid-State Lett.* 5 (2002) A70–A73.
- [22] T. Takeuchi, H. Sakaebe, H. Kageyama, H. Senoh, T. Sakai, K. Tatsumi, *J. Power Sources* 195 (2010) 2928–2934.
- [23] Y. Yang, M.T. McDowell, A. Jackson, J.J. Cha, S.S. Hong, Y. Cui, *Nano Lett.* 10 (2010) 1486–1491.